Study of Corrosion Resistance and Microstructure of the 0.45 wt% C Steel Modified by Pulsed High Energy Density Plasma

K. Wei, Y. Fu, X. Wu, S.-Z. Yang and B. Li

(Submitted 2 September 1998; in revised form 22 January 1999)

A 0.45 wt% C steel was modified by pulsed high energy density plasma (PHEDP), which was composed of particles of aluminum and nitrogen. A layer of thin film was formed on it. The modified steels were studied by an electrochemical corrosion test and transmission electron microscope (TEM) observations. Results showed that the corrosion resistance ability of 0.45 wt% C steel improved after modification, and the film was composed of nanocrystal-aluminum-nitride-phase (AlN), with crystal size of less than 20 nm. The nanocrystal-structured film contributes to the improvement of the corrosion resistance. The improvement is not only related to the microstructure of the film but also to its surface morphology, and both are controlled by the parameters of the PHEDP.

Keywords aluminum nitride, carbon steel, nanocrystals, surface modification

1. Introduction

The improvement of the corrosion resistance and mechanical properties of steel surfaces is an important way to extend steel life. Nitriding treatment of steel surfaces has been used to improve the corrosion and fatigue resistance ability of steel for decades (Ref 1). Recently, nitride films, such as titanium nitride (TiN), aluminum nitride (AlN), and chromium nitride (CrN), have also been deposited on the steel surface by various surface modification methods to improve the corrosion resistance of steel surfaces (Ref 2). Aluminum nitride film is insulating material with high chemical stability, which explains its wide use in functional coatings and devices. It has high corrosion resistance against oxidation in molten aluminum alloys up to 700 °C; therefore, it is used as an anticorrosive coating (Ref 3). It has been deposited by various surface modification methods (Ref 4, 5). However, in all the previously mentioned methods, the heating of the substrate to high temperature, to strengthen the adhesion of the film to the substrate, may cause changes in the structure and properties of the substrate material. As a result some surface modification methods, not involving heating the substrate, have been developed; pulsed high energy density plasma (PHEDP) surface modification is one of them.

Pulsed high energy density plasma has been used to form films, such as titanium carbonitride (TiCN) film (Ref 6) and cubic boron nitride (CBN) film (Ref 7) etc. In PHEDP surface modification, it is not necessary to heat the substrate to strengthen the adhesion between the film and the substrate because the plasma can heat the surface of the substrate to 1500 °C very quickly, changing it into molten state without altering the general characteristics of the steel. The molten surface cools rapidly if the substrate material has good thermal conductivity (such as steel), and the cooling rate can reach 1.01×10^8 °C/s, which is much higher than what is needed in steel quenching (Ref 6). The quenching process of PHEDP is accompanied by the implantation of active plasma particles.

K. Wei, Y. Fu, and **X. Wu,** University of Science and Technology Beijing, Beijing 100083, China; and **S.-Z. Yang** and **B. Li,** Institute of Physics, Chinese Academic of Science, Beijing 100080, China. Contact e-mail: weik@bltda.com.bta.net.cn.

2. Experimental Details

Figure 1 schematically shows the process of PHEDP surface modification. The operating gas is introduced through an electromagnetic valve, and the operating voltage is maintained across the outer and inner aluminum electrodes. Once the gas flows into the coaxial gun, it breaks down. Large current flows through the end of the coaxial gun, which helps the generation of the metal particles by sputtering and evaporation. The plasma, created by the discharge and composed of particles of aluminum and nitrogen, is heated by the Joule heating and accelerated by the Lorentz force, $J \times B$, to the sample.

Disk specimens (22×7 mm diameter) of 0.45 wt% C steel were impacted by PHEDP. Table 1 lists the parameters of PHEDP treatment. Sample 1 was unmodified 0.45 wt% C steel. Samples 2 and 3 were PHEDP modified 0.45 wt% C steel. Each sample was cut into four parts: two of the four parts were used for a corrosion test, and the parts that remained were used for

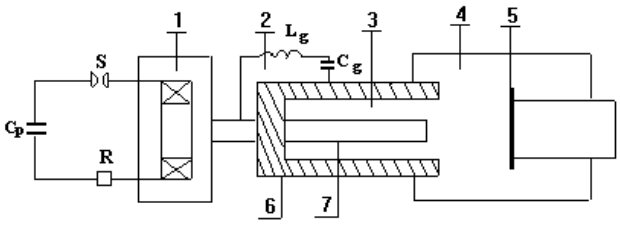

Fig. 1 Diagram of generating pulsed plasma and surface processing. (1) Electromagnetic valve. (2) Charging and discharging circuit. (3) Coaxial plasma gun. (4) Vacuum chamber. (5) Sample holder. (6) Outer electrode. (7) Inner electrode

preparation of the transmission electron microscope (TEM) specimen observation.

The specimens, used in the corrosion test, were prepared as follows: One face of each part of sample 1 was arbitrarily chosen for the corrosion test. Other faces were coated with epoxy. The faces with film of samples 2 and 3 were left for the corrosion test, and the other faces were coated with epoxy. In this experiment the faces left for the corrosion test had an equal area of 1 by 1 mm. These epoxy-coated-samples underwent an electrochemical corrosion test in which Tafel curves of the samples were obtained (Ref 8). The tests were performed on an M351 potentiostat instrument that was in conjunction with a computer and an *x-y* recorder to plot Tafel curves. The corrosion solution was 2 vol% NaCl water. Tafel curves were obtained by recording corrosion current density versus corrosion potential in the range of ±100 mV around the free corrosion potential.

The parameters obtained in the corrosion resistance test of the samples were free corrosion potentials, E_{corr}, and corrosion current density, i_k. The free corrosion potential was measured at the beginning of corrosion test, while the corrosion current density was obtained by computer simulation (shown in Fig. 2).

Transmission electron microscopy specimens were prepared by the cross section method (as shown in Fig. 3). The film sides were glued together, then the glued bulk was cut into slices of 0.5 mm thickness by electric spark machining, and the slices were mechanically abraded to 50 μm thickness followed by argon milling. The TEM observation was performed on a JEOL 100CX (JEOL Ltd.).

3. Results

The results of the corrosion test are shown in Fig. 2 and Table 2. Figure 2 shows the Tafel curves of sample 1 (curve a), sample 2 (curve b), and sample 3 (curve c), and Table 2 shows the values of E_{corr} and i_k and the surface appearance of the samples. The value of E_{corr}, which is related to the Gibbs free energy, stands for resistance ability against the beginning of corrosion. Phases with high Gibbs free energy have a relatively positive value of E_{corr}, thus, high resistance ability. The value of i_k stands for corrosion rate, and a small value of i_k implies low corrosion rate (Ref 8). In Table 2, it can be seen from the appearance of the corroded sample that sample 1 has been corroded more severely than samples 2 and 3. Samples 2 and 3, whose corrosion current densities are about 70% and 45% of that of sample 1, respectively, have lower corrosion rates com-

Table 1 Parameters of the pulsed high energy density plasma (PHEDP) processing

Series No.	Substrate material	PHEDP modified (or unmodified)	Parameters of PHEDP treatment		
			Discharge voltage, kV	Nitrogen pressure, kg/cm^2	Pulse number
Sample 1	0.45 wt% C steel	Unmodified	…	…	…
Sample 2	0.45 wt% C steel	Modified	3.5	2.0	1
Sample 3	0.45 wt% C steel	Modified	0.5	3.0	60

Table 2 Results of the electrochemical corrosion tests of samples 1, 2, and 3

Sample	E_{corr}, mV	i_k A/cm2	Surface appearance	
			Before corrosion test	After corrosion test
Sample 1	–477.0	1.41×10^{-5}	Smooth	A lot of corroded specks at the surface
Sample 2	–499.0	1.00×10^{-5}	Rough	Some corroded specks at the film surface
Sample 3	–442.4	6.60×10^{-6}	Smooth	One or two very small corroded specks at the film surface

Sample 1, 0.45 wt% C steel unmodified; sample 2, 0.45 wt% C steel modified by pulsed high energy density plasma; sample 3, 0.45 wt% C steel modified by pulsed high energy density plasma, 0.5 kV.

Table 3 Indexing of the diffraction pattern of Fig. 4

Ring No.	Ring diameter 2r, mm	Experimental values of d, nm	AIN (hexagonal)	
			Standard values of *d*, nm	*h k l*
1	15.0	0.271	0.2700	100
2	17.5	0.233	0.2372	101
3	21.5	0.189	0.1829	102
4	26.0	0.157	0.1557	110
5	28.0	0.145	0.1414	103
6	30.0	0.136	0.1348	200

$L\lambda$ = 2.035 nm · mm. *d* is the crystal space distance, the experimental values of which were calculated according to $rd = L\lambda$. The standard values of *d* were from JCPDS card (25-1133).

pared with sample 1. Sample 3 has a more positive E_{corr} value than sample 1, while sample 2 has a relatively negative E_{corr} value compared with sample 1. This is because sample 2 has a rough film surface, which is easily corroded because the uneven sites at the surface favor the beginning of corrosion and the formation of corrosion pits. Sample 3 has superior corrosion resistance compared with sample 2. Generally, the PHEDP surface modification can improve the corrosion resistance of 0.45 wt% C steel, but the improvement is resistant by the parameters of PHEDP, as shown in Table 1. The rough surface of sample 2 is caused by the high discharge voltage, which is much higher than that for sample 3. An additional reason that the protective effects of sample 2 are not as effective as those of sample 3 is that the film of sample 2 with one pulse is much thinner than that of sample 3 with 60 pulses.

Figure 4 shows the results of the TEM observations. Figure 4(a) is the diffraction pattern from the film area of sample 2 and sample 3. Indexation of the pattern shows that the diffraction is from aluminum nitride phase. Table 3 shows the result of the indexing. Figure 4(b) is the central dark field image taken with a 101 type reflection of aluminum nitride of the film of samples 2 and 3. It was shown that the particle size of aluminum nitride in the film is smaller than 20 nm.

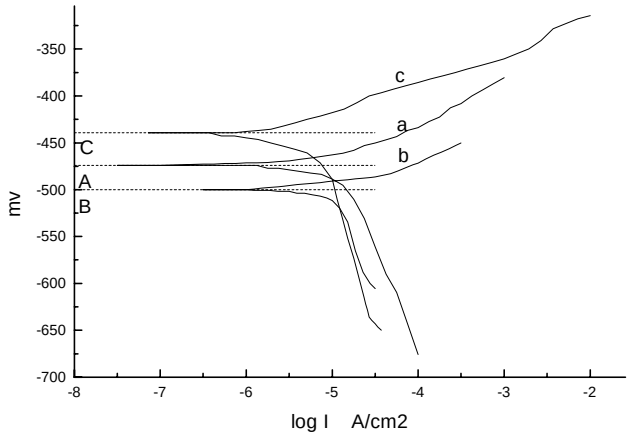

Fig. 2 Tafel curves of samples. (a) Sample 1 (unmodified 0.45 wt% C steel). (b) Sample 2 (0.45 wt% C steel modified by pulsed high energy density plasma, or PHEDP, 3.5 kV). (c) Sample 3 (0.45 wt% C steel modified by PHEDP, 0.5 kV). The ordinates of the points A, B, and C are the values of E_{corr} of samples 1, 2, and 3, respectively.

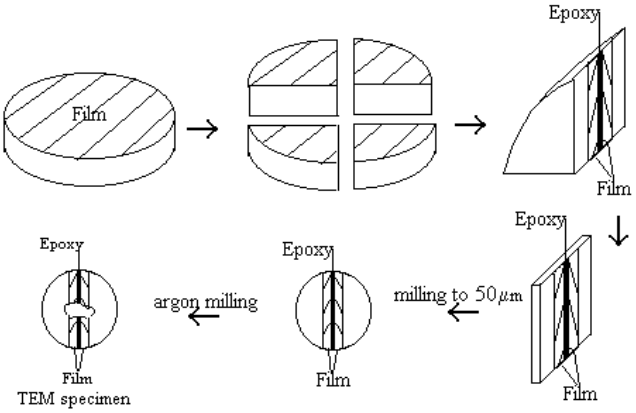

Fig. 3 Schematically shown is the process of specimen preparation for transmission electron microscopy observation.

4. Discussion

The electrochemical corrosion of steel is usually produced by the formation of microcorrosion cells caused by the potential difference among sites of the steel surface due to the heterogeneity of the microstructure, composition, or stress. The electrochemical corrosion reaction in neutral solution is (Ref 9):

$$\text{Anodic reaction } Fe \rightarrow Fe^{2+} + 2e \qquad \text{(Eq a)}$$

$$\text{Cathodic reaction } (1/2)O_2 + H_2O + 2e \rightarrow 2OH^- \qquad \text{(Eq b)}$$

In the anodic reaction, iron atoms lose electrons and dissolve into the solution.

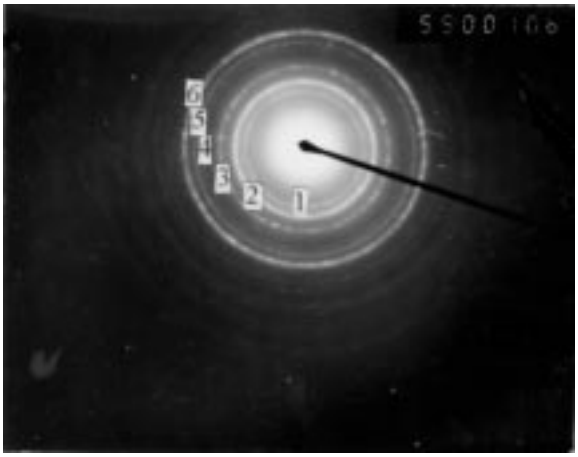

(a)

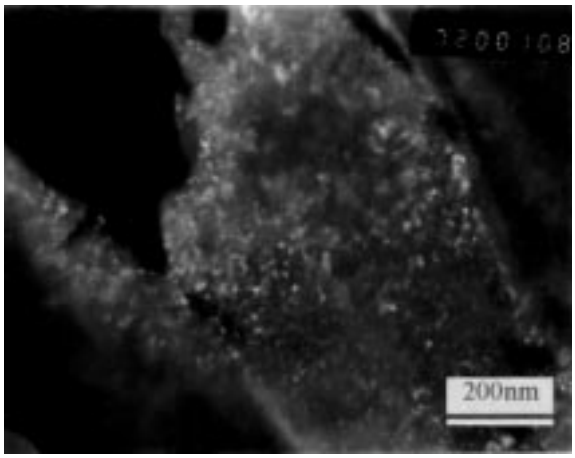

(b)

Fig. 4 (a) Selected area diffraction pattern (SAD) from the phases in film of samples 2 and 3. (b) Central dark field image (CDF) of AIN phase taken by type 101 diffraction in the pattern of Fig. 4(a)

The 0.45 wt% C steel, which is composed of ferrite (α-Fe) and cementite (Fe_3C), has poor corrosion resistance because it easily forms microcorrosion cells due to the potential difference between the two phases. After being modified by PHEDP, the surface of 0.45 wt% C steel is protected by a layer of dense aluminum nitride film, which is free from the formation of microcorrosion cells by phase heterogeneity. Aluminum nitride has a high Gibbs free energy (approximately –316 kJ/mol, Ref 10), which makes it stable during chemical reactions, as identified in the corrosion test. In addition, the aluminum nitride phase formed by PHEDP has a nanocrystalline structure, which shows abnormal performances of some properties compared with conventional polycrystalline structure. The ratio of interfacial area to the grain volume of nanocrystalline material is relatively large. It has been shown that the intercrystalline (grain boundary and triple junction) content of material increases from a value of 0.3% at a grain size of 1μm to more than 50% at grain sizes less than 5nm (Ref 11). Therefore, the nanocrystalline material has evenly distributed defect sites (e.g., grain boundary) and corrodes uniformly on the surface. Furthermore, the energy of the grain boundaries of nanocrystals is low and, thus, not so active as that of conventional polycrystalline structures (Ref 12, 13). It has been proved that nanocrystalline materials have superior localized corrosion resistance compared with the conventional polycrystalline materials, even though the composition of both is the same (Ref 14, 15). Consequently, the nanostructured aluminum nitride film has high corrosion resistance, which prevents the electrochemical reaction between the steel and the solution and improves the corrosion resistance of the 0.45 wt% C steel. The corrosion resistance is not only related to the surface microstructure, but also to the surface morphology, as shown in Table 2. The corrosion resistance of sample 3 with a smooth film surface is better than that of sample 2 with a rough film surface.

The microstructure and morphology of the surface of film are related to the energy density of the plasma, which increases with the discharge voltage. High energy density plasma produced under high discharge voltage can heat the modified surface into a molten state and result in high cooling rate; thus, the nucleation rate on the surface is rapid enough for the formation of nanocrystals. Accordingly, high discharge voltages prefer the formation of nanostructured aluminum nitride films but often with a rough surface; low discharge voltages favor the formation of smooth surfaces but are unfavorable for the formation of aluminum nitride. Therefore the selection of the discharge voltage of PHEDP is one of the key elements for producing good film. The most suitable condition for the formation of an aluminum nitride film with a high corrosion resistance was found to be 0.5 kV in this experiment.

5. Conclusions

From the results stated in this article, the following conclusions can be established:

- The 0.45 wt% C steel modified by PHEDP has improved corrosion resistance in 2 vol% NaCl solution.
- Transmission electron microscopy studies show that the film is composed of a nanometer-sized aluminum nitride phase.
- The improvement of anticorrosion ability of 0.45 wt% C steel is due to the formation of the dense aluminum nitride film, which is resistant to the formation of microcorrosion cells in solution and has a more positive E_{corr} value and lower corrosion rate than 0.45 wt% C steel.
- The corrosion resistance of the film is also related to its surface state. Sample 3 with smooth film has better corrosion resistance ability than sample 2 with a rough film.
- High discharge voltages prefer to form adhesive but rough aluminum nitride films, while too low discharge voltages are unfavorable to the formation of aluminum nitride films. A well-selected discharge voltage is an important element for producing good anticorrosion films.

Acknowledgment

The authors would like to acknowledge the financial support provided by the National Nature Science Foundation of China and International Atomic Energy Agency.

References

1. H.V. Boening, Additional Application of Plasma Science, *Plasma Science and Technology,* Cornell University Press, 1982, p 266
2. D.M. Mottox, J.E. Greene, D.H. Bucley and G.A. Somorjai, Properties of Coated and Modified Surface, *Mater. Sci. Eng.*, Vol 70, 1985, p 79-89
3. Y.G. Roman and A.P.M. Adriaansen, Aluminum Nitride Films Made by Low Pressure Chemical Vapor Deposition: Preparation and Properties, *Thin Solid Films*, Vol 169, 1989, p 241-248
4. R. Macmahon, J. Affimito, and R. Parsons, Voltage Controlled Reactive Planar Magnetron Sputtering of AlN Thin Film, *J. Vac. Sci. Technol.*, Vol 20, 1982, p 376
5. G. Este, R. Surridge, and W.D. Westwood, Reactively Sputtered AlN Films for GaAs Annealing Caps, *J. Vac. Sci. Technol. A*, Vol 4 (No. 3), 1986, p 989
6. P.X. Yan, S.Z. Yang, and X.S. Chen, A New Technique for Deposition of Titanium Carbonitride Films at Room Temperature by High Energy Density Pulse Plasma, *Nuclear Instrument and Methods in Physics Research*, Vol B00, 1994
7. P.S. Yan, S.Z. Yan, B. Li and X.S. Chen, Pulsed Plasma Deposition of C-BN Thin Films on Silicon Substrate, *Phys. Status Solidi (a)*, Vol 145, 1994, p K29
8. L.L. Shreir, Ed., Standard Chemical Potentials, *Corrosion*, George Newnes Ltd., London, 1983, p 21.10
9. *Corrosion, ASM Handbook*, 9th ed., L.J. Korb and D.L. Olson, Ed., ASM International, 1987, p 511
10. S.L. Wei and S. Bai, Substance Index, *Wujiwu Relixue Shuju Shouce*, Northeast University Press, 1993, p 51 (in Chinese)
11. G. Paulumbo, S.J. Thorpe and K.T. Aust, On the Contribution of Triple Junctions to the Structure and Properties of Nanocrystalline Materials, *Scr. Metall. Mater.*, Vol 24, 1990, p 1347-1350
12. G.J. Thomas, R.W. Siegel and J.A. Eastman, Grain Boundaries in Nanophase Palladium: High Resolution Electron Microscopy and Image Simulation, *Scr. Metall. Mater.*, Vol 24, 1990, p 201
13. J. Wang, D. Wolf and S.R. Phillpot, Computer Simulation of the Structure and Thermal-Elastic Properties of a Model Nanocrystalline Material, *Philos. Mag. A*, Vol 73, 1996, p 517
14. L. Ke and Z. Fei, Recent Research Progress on Nanocrystalline Materials, *Acta Metall. Sini.*, Vol 33, 1997, p 99-106
15. R.B. Inturi and Z.S. Smialowska, Localized Corrosion of Nanocrystalline Stainless Steel Films, *Corrosion*, Vol 48 (No. 5), 1992, p 398-403